ENVIRONMENTAL RESEARCH
LETTERS

PURPOSE-LED PUBLISHING™

Celebrating the 20th anniversary of Environmental Research Letters

LETTER • OPEN ACCESS

Impacts of land-use change on century-scale global soil NO_x emissions using the biogeochemical model VISIT

To cite this article: Kazuya Nishina *et al* 2026 *Environ. Res. Lett.* **21** 104023

View the article online for updates and enhancements.

You may also like

- Asian zonal-dipole climate extremes in 2022 and 2025: role of upper-tropospheric zonal flow
Chao He, Tianjun Zhou, Peili Wu et al.
- Corn–soybean expansion nears threshold for adverse nitrogen effects in the Great Plains
Breanna Rivera Waterman, Amy T Hansen, Terrance D Loecke et al.
- Incorporating plastic pollution into the global change framework
Austin Gray and Rachel Leads

This content was downloaded from IP address 192.17.106.135 on 01/07/2026 at 22:50

ENVIRONMENTAL RESEARCH
LETTERS

Check for updates

OPEN ACCESS

RECEIVED
16 March 2026

REVISED
16 April 2026

ACCEPTED FOR PUBLICATION
12 May 2026

PUBLISHED
21 May 2026

Original content from this work may be used under the terms of the Creative Commons Attribution 4.0 licence.

Any further distribution of this work must maintain attribution to the author(s) and the title of the work, journal citation and DOI.

LETTER

Impacts of land-use change on century-scale global soil NOx emissions using the biogeochemical model VISIT

Kazuya Nishina[1,*], Akihiko Ito[1,2], Hanqin Tian[3], Tatsuya Nagashima[1], Yuto Osugi[4], Naiqing Pan[3], Shufen Pan[3,10], Sian Kou-Giesbrecht[5], Federico Maggi[6], Atul K Jain[7], Nicolas Vuichard[8] and Sönke Zaehle[9]

[1] Earth System Division, National Institute for Environmental Studies, 16-2, Onogawa, Tsukuba, Ibaraki 305-8506, Japan
[2] Graduate School of Agricultural and Life Sciences, The University of Tokyo, 1-1-1, Yayoi, Bunkyo-ku, Tokyo 113-8657, Japan
[3] Center for Earth system Science and Global Sustainability, Department of Earth and Environmental Sciences, Boston College, Chestnut Hill, MA 02467, United States of America
[4] Department of Environmental Engineering, Graduate School of Engineering, Kyoto University, Kyoto 615-8540, Japan
[5] School of Resource and Environmental Management, Simon Fraser University, Burnaby, British Columbia, Canada
[6] School of Civil Engineering, The University of Sydney, Darlington NSW 2008, Australia
[7] Department of Climate, Meteorology and Atmospheric Sciences (CLiMAS), University of Illinois, Urbana, IL 61801, United States of America
[8] Laboratoire des Sciences du Climat et de l'Environnement, LSCE-IPSL (CEA-CNRS-UVSQ), Université Paris-Saclay, 91191 Gif-sur-Yvette, France
[9] Department of Biogeochemical Signals, Max Planck Institute for Biogeochemistry, Hans-Knöll-Straße 10, 07745 Jena, Germany
[10] Department of Engineering, Boston College, Chestnut Hill, MA 02457, United States of America
[*] Author to whom any correspondence should be addressed.

E-mail: nishina.kazuya@nies.go.jp

Keywords: soil NOx, land-use change, canopy reduction, fertilizer

Supplementary material for this article is available online

Abstract

Soils represent a significant natural source of nitric oxide (NO), a precursor of nitrogen oxides (NOx) that play an essential role in atmospheric chemistry and radiative forcing. However, historical estimates of global soil NOx emissions have been constrained by limited long-term nitrogen input datasets and methodological gaps in process representation. In this study, we present the first century-scale simulation of global soil NOx emissions (1850–2020) using the biogeochemical model VISIT (The Vegetation Integrative SImulator for Trace gases), coupled with the newly developed History of anthropogenic Nitrogen inputs dataset of harmonized anthropogenic nitrogen inputs. Our results reveal that total global soil NOx emissions increased gradually from an average of 22.1 Tg N yr^{-1} prior to 1900 to 25.3 Tg N yr^{-1} in the 2010s, with emissions above the canopy ranging from 12.2 to 13.6 Tg N yr^{-1}. Notably, while soil NOx emissions from natural ecosystems showed a marginal decline, the contribution of agricultural soils experienced a more than fourfold increase to global NOx emissions, driven primarily by fertilizer and manure application since the mid-20th century. This led to a more than fourfold increase in the share of agricultural land in global soil NOx emissions, rising from 7.8% to 31.3%. Regional analysis indicates substantial increases in Europe, Asia, and North America, with soil NOx emissions becoming a dominant source in sparsely populated and arid regions. These findings underscore the growing importance of soil-derived NOx in the global nitrogen budget and its implications for future air quality and climate mitigation strategies. This work provides a robust basis for refining emission inventories and supports the development of region-specific nitrogen management to mitigate unintended NOx emissions from soils. On the other hand, benchmarking against the results in Nitrogen Model Inter-comparison Project (NMIP2) revealed significant divergence in global soil NOx emissions between models, with the VISIT estimates on the higher end, highlighting the urgent need for improved process representation and observational constraints.

© 2026 The Author(s). Published by IOP Publishing Ltd

1. Introduction

Soils are a significant natural source of nitric oxide (NO), a precursor of nitrogen oxides (NO*x*), which contribute to tropospheric ozone (O_3) formation and influence the atmosphere's overall oxidizing capacity (Davidson and Kingerlee 1997). Globally, soil emissions account for approximately 15% of total NO*x* emissions, positioning them as a major component of the atmospheric nitrogen budget alongside fossil fuel combustion (Steinkamp and Lawrence 2011, Miyazaki *et al* 2017). The Intergovernmental Panel on Climate Change underscores the necessity of reducing short-lived climate forcers, including NO*x*, to mitigate climate change impacts (Szopa *et al* 2021).

While fossil fuel-derived NO*x* emissions have shown a declining trend due to air pollution mitigation strategies in some regions (e.g. Christiansen *et al* 2024, Chatani *et al* 2025), the relative importance of soil-derived NO*x* is expected to increase (Song *et al* 2021). This shift is further driven by the continued rise in nitrogen fertilizer application since the Industrial Revolution (Tian *et al* 2022). Understanding the balance of reactive nitrogen in the atmosphere—including NO*x* fluxes—is critical not only for evaluating radiative forcing but also for guiding effective climate mitigation strategies (Gong *et al* 2024).

In rural and agricultural regions, soil NO*x* emissions can dominate local NO*x* budgets, particularly under specific seasonal or management conditions (Oikawa *et al* 2015, Almaraz *et al* 2018, Sha *et al* 2021, Skiba *et al* 2021). These emissions enhance surface O_3 levels, which pose substantial risks to vegetation, including yield reductions in crops and impaired forest productivity (e.g. Gregg *et al* 2003, Feng *et al* 2008). Elevated O_3 levels disrupt photosynthesis, reduce chlorophyll concentration, and accelerate leaf senescence, ultimately impairing agricultural productivity (Ainsworth and Long 2005). Consequently, regulating soil NO*x* emissions is essential to safeguarding ecosystem health and food security. However, in real atmospheric environments, the relationship between NO*x* and ground-level O_3 is complex, and it is important to note that, under volatile organic carbon-limited (NO*x*-saturated) regimes, reducing NO*x* emissions may paradoxically lead to increases in O_3 concentrations through reduced titration of O_3 by NO and altered photochemical balance (Atkinson 2000).

NO production in soils arises from complex interactions of biotic and abiotic processes, mainly microbial nitrification and denitrification. Nitrification aerobically oxidizes ammonium (NH_4^+) to nitrate (NO_3^-), while denitrification anaerobically reduces NO_3^- to nitrogen gas (N_2), with NO as a key intermediate (Pilegaard 2013). These processes are modulated by environmental factors including nitrogen availability, soil moisture, temperature, oxygen concentration, pH, and organic matter content (Nishina *et al* 2009, 2012, Pilegaard 2013). For example, in a study by Steinkamp and Lawrence (2011), differences in estimation methods resulted in widely varying estimates of global annual soil NO*x* emissions, ranging from 10 to 33 $Tg\,N\,yr^{-1}$ (Steinkamp and Lawrence 2011), a large and significant magnitude relative to the uncertainties associated with global N_2O emission estimates (Tian *et al* 2020).

Understanding long-term changes in soil NO*x* emissions is essential for assessing the impacts of nitrogen enrichment on atmospheric chemistry and ecosystem processes. Previous global estimates, however, have been largely limited to short-term windows (e.g. Yienger and Levy 1995), primarily due to the lack of harmonized nitrogen input data over historical time sequences. This has constrained our ability not only to examine long-term trends accompanied with land-use change but also to account for the spatial and seasonal heterogeneity in soil NO*x* fluxes, which are increasingly recognized as critical factors influencing radiative forcing and tropospheric chemistry. For example, Derwent *et al* (2008) demonstrated that the climate impacts of surface NO*x* emissions vary substantially by region and season due to nonlinear interactions with methane and ozone, resulting in radiative forcing effects that differ markedly across emission scenarios. These findings underscore the need to resolve both the temporal evolution and spatial diversity of soil NO*x* emissions when evaluating their cumulative climate effects. In this study, we leverage the newly developed History of anthropogenic Nitrogen inputs (HaNi) dataset (Tian *et al* 2022), which provides consistent, high-resolution nitrogen input estimates from preindustrial era to the present. By coupling HaNi with historical land-use and climate data, we present—for the first time—a century-scale simulation of global soil NO*x* emissions. This framework enables a more robust understanding of the long-term atmospheric and ecological consequences of reactive nitrogen dynamics.

To advance understanding of the long-term contribution of soil NO*x* emissions, we incorporated an established soil NO*x* emission scheme (Parton *et al* 2001) into the global terrestrial biogeochemical model VISIT (The Vegetation Integrative SImulator for Trace gases) (Ito and Inatomi 2011). Biogeochemical models are superior to empirical models in handling the temporal changes in nitrogen cycles containing carbon within ecosystems with time evolution (e.g. seasonal and long-term changes in biomass or land-use changes). Our study provides historical estimates of global soil NO*x* emissions from 1850 to 2020 and evaluates their associated uncertainties using results and inventories from the

2nd Global Nitrogen/N_2O Model Intercomparison Project (NMIP). This integrative approach enables a comprehensive assessment of both the significance and challenges of soil NO*x* emissions.

2. Materials and methods

2.1. Model description: VISIT

VISIT is a process-based terrestrial ecosystem model developed for the trace gas emissions at the global scale (Ito and Inatomi 2011, Ito 2018, 2019). VISIT simulates carbon, nitrogen, and water cycles within terrestrial ecosystems, focusing on trace gas exchange between the atmosphere and the biosphere. It operates globally with a spatial resolution of $0.5° \times 0.5°$, using inputs such as climate variables, atmospheric CO_2 concentrations, N deposition, and land-use data to simulate ecosystem processes. For cropland, N fertilizer and manure application rates are used as input data. The model has been validated extensively across various scales, demonstrating its capability to represent ecosystem functions. Previous studies using VISIT have evaluated greenhouse gas exchanges including CO_2, CH_4, and N_2O, providing insights into the impacts of environmental change on these fluxes (Ito 2018, 2019).

The original VISIT model has not been incorporated into the soil NO*x* emission scheme. Because the N_2O process in the VISIT model is based on the DAYCENT model (Parton *et al* 1996), we newly incorporated the scheme for soil NO*x* emissions for DAYCENT model (Parton *et al* 2001). This scheme simulates soil NO fluxes from nitrification and denitrification as functions of soil moisture, temperature, nitrogen availability, and gas diffusivity (Parton *et al* 2001).

N_2O emissions derived from nitrification (fN_2O_{nit}) and denitrification (fN_2O_{den}) processes in the VISIT model are formulated using the following equations:

$$fN_2O_{nit} = f_{nit}(\mathrm{WFPS}) \cdot f_{nit}(\mathrm{pH}) \cdot f_{nit}(\mathrm{temp}) \left(K_{max} + F_{max} \cdot NH_4^+\right), \quad (1)$$

$$fN_2O_{den} = \frac{f_{den}(\mathrm{WFPS}) \cdot \min\left[f_{den}(N_{NO_3}),\, f_{den}(\mathrm{HR})\right]}{1.0 + R_{N_2/N_2O}}. \quad (2)$$

In equation (1), f_{nit}(WFPS), f_{nit}(pH), and f_{nit}(temp) represent the dependency of nitrification rates on water-filled pore space (WFPS), soil pH, and temperature, respectively. The combined potential of N_2O production from nitrification is further determined by a base turnover coefficient (K_{max}) and an ammonium-dependent flux term ($F_{max} \cdot NH_4$), where NH_4^+ represents the concentration of ammonium in the soil.

The response function for the denitrification process to WFPS is indicated by f_{den}(WFPS) (equation (2)). The substrate limitation is determined by the minimum of two functions, $f_{den}(N_{NO3})$ and f_{den}(HR), where the former accounts for the effect of nitrate availability and the latter reflects the influence of heterotrophic respiration as a proxy for carbon substrate supply. The entire expression is divided by $1.0 + R_{N_2/N_2O}$, where R_{N_2/N_2O} is the ratio of molecular nitrogen (N_2) to nitrous oxide (N_2O) among the denitrification products.

Based on the N_2O emissions, NO*x* emission rates are estimated by the NO:N_2O ratio defined by the following equation (Parton *et al* 2001):

$$R_{NO} = 15.2 + \frac{(35.5 \arctan(0.68\pi(10D/D_0 - 1.86)))}{\pi}, \quad (3)$$

where R_{NO} is the ratio of NO to N_2O fluxes and D/D_0 is the soil gas diffusivity. Furthermore, the relationship between soil moisture content and D/D_0 varies with soil texture (from sandy loam to clay loam), as described in Parton *et al* (2001). Sandy loam exhibits a higher D/D_0 for the same moisture content than other soil textures. Since the VISIT model is a monthly calculation step, the function related to a spike in NO emissions in denitrification induced by heavy rainfall on dry soil in the original model (Parton *et al* 2001) has been omitted. Therefore, soil NO emissions in the VISIT model are defined as follow:

$$fNO_{soil} = R_{NO} * (fN_2O_{nit} + fN_2O_{den}). \quad (4)$$

As described above, only NO is directly emitted from the soil; however, once released into the atmosphere, NO is rapidly oxidized to NO_2 (Atkinson *et al* 2004), meaning that the flux from the canopy includes both NO and NO_2. Therefore, in this study, both NO emissions from the soil surface and the ecosystem (above canopy) are also expressed collectively as NO*x* (NO and NO_2) emissions.

Vegetation canopies substantially attenuate NO emitted from the soil before it reaches the atmosphere. Various physical and chemical processes within the canopy, such as oxidation to nitrogen dioxide (NO_2), deposition onto leaf surfaces, dissolution in atmospheric moisture, and photochemical decomposition, significantly reduce the amount of NO transported to the atmosphere (Jacob *et al* 1995, Ganzeveld *et al* 2002). Empirical studies indicate that canopy uptake can greatly diminish soil-emitted NO fluxes, resulting in lower NO*x* concentrations observed above the canopy than the

fluxes directly measured at the soil surface (Jacob *et al* 1995). Incorporating such canopy-reduction effects into atmospheric models enhances the accuracy of predicting atmospheric NO*x* concentrations and improves our understanding of nitrogen cycling within terrestrial ecosystems (Ganzeveld *et al* 2002, Yan *et al* 2005). Therefore, we have introduced the canopy reduction factor (CRF) to estimate above-canopy NO flux (NO_{cnpy}) according to Yienger and Levy (1995). CRF is defined as follows:

$$\mathrm{CRF} = \frac{e^{-k_s \mathrm{SAI}} + e^{-k_c \mathrm{LAI}}}{2}, \quad (5)$$

where SAI and LAI are stomatal area index and leaf area index, respectively, and k_s and k_c are constants, which values used in this study were 8.75 and 0.24, respectively, according to Yienger and Levy (1995). LAI were calculated endogenously in VISIT using the plant biomass scheme in the model. SAI in each vegetation type was obtained from Yienger and Levy (1995). Each SAI value corresponds to the vegetation type described in the Olson biome types implemented in VISIT and ranged from 0.010 to 0.120

$$f\mathrm{NO}_{\mathrm{cnpy}} = f\mathrm{NO}_{\mathrm{soil}} \times \mathrm{CRF}, \quad (6)$$

where $f\mathrm{NO}_{\mathrm{cnpy}}$ indicates ecosystem NO*x* emissions, which are the NO*x* emissions from the canopy surface after the attenuation by canopy reduction.

Note that NO absorbed by the forest canopy (i.e. NO $\times$ (1 $-$ CRF)) is returned back to the soil as inorganic nitrogen by rainfall and litter-fall in the VISIT model.

2.2. Simulation settings

The simulation settings in this study is according to Nitrogen Model Inter-comparison phase 2 (NMIP2) protocol provided by Sun *et al* (2024). The simulation period was from 1850 to 2020. The spatial resolution was half degree at global. The climate forcing was based on the CRU-JRA v2.2 dataset for the period 1901–2020 (Harris 2021). Atmospheric CO_2 concentrations were prescribed using ice core records and NOAA observations spanning 1850–2020 (Joos and Spahni 2008, Lan *et al* 2023). Land-use and land-cover changes were provided by the land-use Harmonization dataset version 2 (LUH2), also covering 1850–2020 (Hurtt *et al* 2020).

This study used the scenario with full anthropogenic N inputs (called SH1 in NMIP2 protocol). Nitrogen deposition inputs were derived from the IGAC/SPARC Chemistry-Climate Model Initiative (CCMI) simulations (Hegglin *et al* 2016). Anthropogenic nitrogen inputs via fertilizer and manure were obtained from the HaNi (Harmonized Anthropogenic Nitrogen input) dataset (Tian *et al* 2022), with fertilizer data available from 1911 and manure data from 1850 onward. LUH2 also provides irrigation areas in cropland (Hurtt *et al* 2020). For model spin-up, climate data from 1901 to 1920 were recycled repeatedly, and a control simulation using fixed boundary conditions was performed to verify equilibrium (Sun *et al* 2024). VISIT without soil NO*x* scheme has previously participated in the Nitrogen Model Intercomparison Project phase (NMIP2) under harmonized forcing datasets (Tian *et al* 2024). The present study extends this framework by introducing a soil NO*x* emission scheme.

2.3. Contribution of soil NO*x* emission to total anthropogenic NO*x* emissions in land

We evaluate the relative contributions of soil NO*x* emissions to total land NO*x* emissions. For the land emissions, we used the EDGAR HTAP v3 database developed by Crippa *et al* (2023). To calculate the total NO*x* emissions from land surfaces for EDGAR HTAP v3 database except soil NO*x* emission, we excluded the NO*x* emissions in '1. international shipping', '2.1 domestic aviation', '2.2 international aviation', '5.3 domestic shipping', and '8.3 agriculture crops' from total sum of NO*x* emission. Then, to calculate the contribution of each grid to soil NO*x* emissions (above canopy) simulated by VISIT, the contribution was calculated as Soil NO*x*/(Soil NO*x* + land NO*x*).

2.4. Soil NO*x* emissions in NMIP2 models for benchmark

We used the simulation results of terrestrial biosphere models from NMIP2 study (Sun *et al* 2024, Tian *et al* 2024) with the NO flux outputs, which were BRTSim-BAMS4 (Pasut *et al* 2021), CLASSIC (Melton *et al* 2020, Kou-Giesbrecht and Arora 2023), DLEM (Tian *et al* 2015, Xu *et al* 2017), ISAM (Shu *et al* 2020), O-CN (Zaehle and Friend 2010), ORCHIDEE (Vuichard *et al* 2019). All models were simulated under the NMIP2 protocol.

3. Results and discussions

3.1. Overall historical trend in global soil NO*x* emission

Global total soil NO emissions in VISIT have shown an increasing trend from 1850 to 2020, with a minimum value of 20.1 Tg N yr^{-1} in 1850 and a maximum value of 27.0 Tg N yr^{-1} in 2010 (figure 1). Considering the attenuation by vegetation canopy, the range of emissions for the entire period was 10.6 Tg N yr^{-1} to 14.8 Tg N yr^{-1} (figure 1(left)). Global hotspots for soil NO*x* emissions (for the year 2000) were found in the Corn Belt of North America, tropical rainforest regions, and South and East Asia. Additionally, high emissions were observed in the

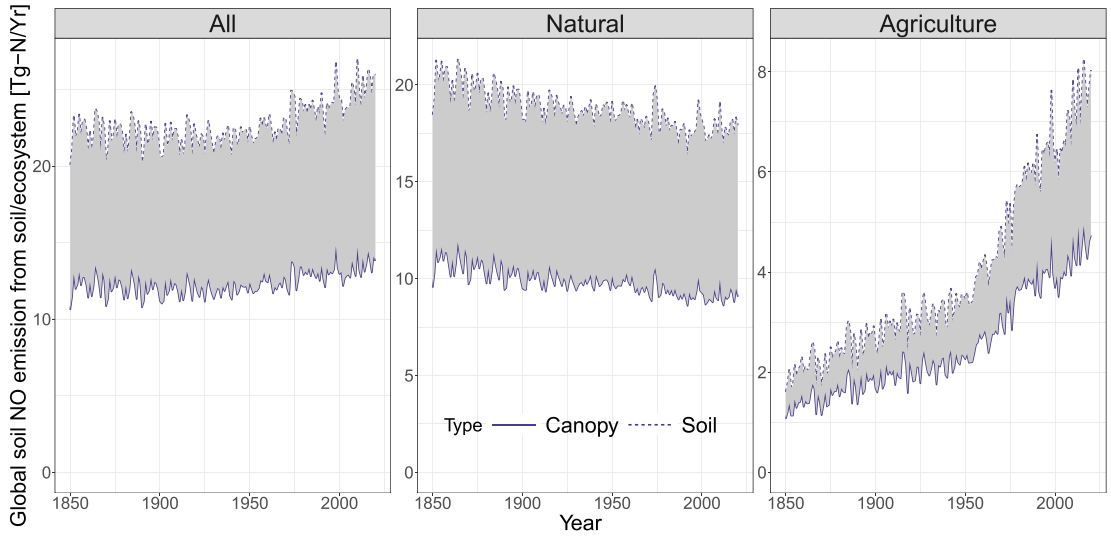


Figure 1. Time series of global soil NO*x* emissions from the soil surface and vegetation canopy in VISIT. Overall and for natural ecosystems and agricultural ecosystems. Gray areas indicates the amount of reduction by canopy attenuation.

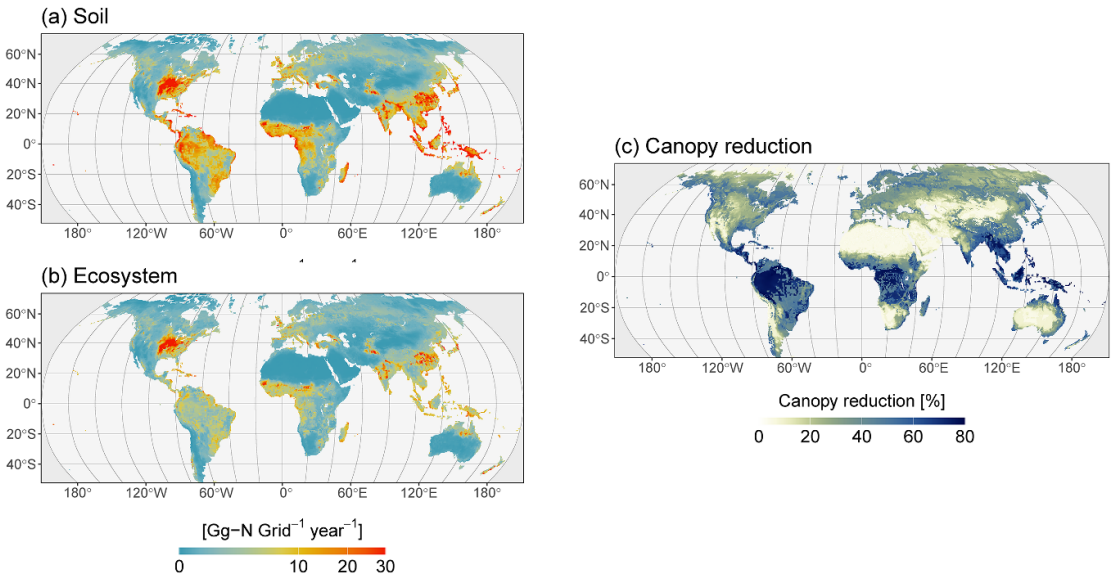


Figure 2. Map of soil NO*x* emissions from the soil surface (upper) and above forest canopy (below) in 2010. The middle map shows the fraction of the reduction in soil NO*x* emission by canopy attenuation (i.e. CRF).

grain-producing regions extending from Europe to Eurasia (figure 2).

Compared with previous estimates, global soil NO*x* emissions estimated in this study were within the range of previous studies but were above average (table 1). Some studies have referenced the highly influential pioneering empirical model (YL95) developed by Yienger and Levy (1995), while process models that calculate ecosystem carbon and nitrogen budgets, such as the one used in this study, are three examples in table 1. (Potter *et al* 1996, Tao and Jain 2005, Zaehle and Friend 2010). The differences in the estimates are attributed to various factors, including the computational approach, resolution, handling of fluxes immediately after rainfall, and the level of detail in ecosystem classification. However, the most significant difference between this study and most of the previous studies appears to be the treatment of nitrogen deposition and manure inputs. In previous studies, these nitrogen flows were not explicitly considered except in (Hudman *et al* 2012), but even in the 1990s, the global N loads were approximately 62.4 Tg N yr^{-1} in N deposition and 87.1 Tg N yr^{-1} in manure, respectively (Tian *et al* 2022). These anthropogenic inputs represent significant N loadings contributing to reactive N supply to

Table 1. Estimates of global soil NO*x* emissions from previous studies.

Soil surface ($Tg\,N\,yr^{-1}$)	Above canopy ($Tg\,N\,yr^{-1}$)	Estimation method	Reference year(s)	References
10.2	5.5 (3.3–7.7)	Empirical model (original YL95)	1990s	Yienger and Levy (1995)
9.7	—	Process-based model	1990s	Potter *et al* (1996)
21	13	Inventory using biome-level emission factors	1990s	Davidson and Kingerlee (1997)
12	8	Empirical model (revised YL95)	1990s	Ganzeveld *et al* (2002)
7.4	5.0	Empirical model (revised YL95)	1990s	Yan *et al* (2005)
7.5	—	Process-based model (ISAM model)	2000	Tao and Jain (2005)
35.0/26.8	—	Process-based model (O-C and O-CN models)	1990s	Zaehle and Friend (2010)
33.1/10.5	26.7/8.5	Empirical model (revised YL95)	2000s	Steinkamp and Lawrence (2011)
7.4	6.2	Empirical model (BDSNP model)	2000s	Hudman *et al* (2012)
—	12.9 ± 3.9	Inverse estimate (OMI satellite NO_2 data)	2005–2008	Vinken *et al* (2014)
—	7.9	Inverse estimate	2005–2014	Miyazaki *et al* (2017)
—	9.5	Empirical model (revised YL95)	1990s	Weng *et al* (2020)
—	9.1	Empirical model (revised YL95)	2005	Simpson and Darras (2021)
13.8 (95%C.I.: 9.1–20.7)	9.1 (95%C.I.: 6.6–12.5)	Average for above studies		
24.2 ± 1.3	13.2 ± 0.7	Process-based model	1990s	This study (VISIT)
24.1 ± 0.7	12.9 ± 0.4	Process-based model	2000s	This study (VISIT)
15.0 (95%C.I.: 7.6–29.8)	—	Multi-model ensemble average	1990s	NMIP2
15.2 (95%C.I.: 7.5–29.9)	—	Multi-model ensemble average	2000s	NMIP2

The revised YL95 approach maintains a similar core framework, but specific parameters differ among the revised YL95. The fertilizer-induced emission factor was updated from 2.5% in the original YL95 to lower values based on field observations, such as 1.16% in Yan *et al* (2005), 1.0% in Steinkamp and Lawrence (2011), 1.5% in Hudman *et al* (2012), and 0.7% in Simpson and Darras (2021). Soil moisture parameterizations evolved from discrete wet/dry states based on precipitation history to continuous functions using actual volumetric soil moisture (Hudman *et al* 2012, Weng *et al* 2020). Other changes include the incorporation of additional mechanistic factors, such as soil organic carbon, soil pH (Yan *et al* 2005), and seasonal fertilization (Hudman *et al* 2012).

terrestrial ecosystems. In previous studies, the emission factors of soil NO*x* emissions for manure application were considered to be approximately the same or higher than those for chemical fertilizers (e.g. Bouwman *et al* 2002, Liu *et al* 2017). Therefore, taking these additional nitrogen loads into account, it is likely that the emissions from agricultural land and grassland in particular will be upwardly corrected in each of the estimation methods used in previous studies (Hudman *et al* 2012). Furthermore, Furthermore, unlike process models such as VISIT, empirical models do not address changes in nitrogen pools in each ecosystem over time and, therefore, do not take into account the accumulation (or loss) resulting from these continuous inputs.

In contrast, although global above-canopy NO*x* emissions were higher in this study than in previous studies (table 1), it is worth noting that the values are in a comparable order and fall within the uncertainty range estimated by satellite inversion (Vinken *et al* 2014). A recent EU subcontinental-scale inversion study using TROPOMI satellite NO*x* data reported that the above-canopy NO*x* emissions in the posterior became approximately 1.7 times higher than those in Copernicus Atmosphere Monitoring Service global emission inventories (Simpson and Darras 2021), with particularly large discrepancies over forested area, highlighting the underestimation of NO*x* emissions from ecosystems (Lin *et al* 2024). On the basis of these recent findings, the values obtained in

this study are not considered extremely high and are deemed to represent reasonable estimates.

When considering natural ecosystems alone, soil NO*x* emissions show a slight downward trend over time, with an average of 19.8 Tg N yr^{-1} prior to 1900 and 17.8 Tg N yr^{-1} in the 2000s. Conversely, the emissions from agricultural lands show an increasing trend, and the overall increasing trend is clearly driven by enhanced soil NO*x* emissions from agricultural land, which exceeded the concurrent decrease in natural ecosystem emissions and led to an upward global trend. The significant increasing trend during the calculation period, with the minimum emissions of 1.6 Tg N yr^{-1} in 1850 and maximum emissions of 8.3 Tg N yr^{-1} in 2016, representing an increase of approximately fivefold. The decrease in natural ecosystem-derived soil NO*x* emissions and the increase in agricultural ecosystem emissions are largely attributed to land-use changes from natural ecosystems such as forests and grasslands to agricultural land-use for crop production and grazing (Hurtt *et al* 2020). Although these land-use changes increased approximately linearly from 1850 through the 1980s, their incresing trend has slowed and has largely plateaued since the 1990s (Hurtt *et al* 2020). In contrast, agricultural soil NO_x emissions have exhibited an accelerated upward trend since the 1950s, primarily driven by the increased application of chemical nitrogen fertilizers and manure inputs (Tian *et al* 2022). As a result, the contribution ratio of agricultural land to global soil NO*x* emissions during this calculation period increased sharply from 7.8% to 31.3% (figure 1). In terms of ecosystem NO*x* emissions, due to differences in the extent of canopy attenuation, the contribution of agricultural land can be estimated to be even higher, at 9.3% to 35.0%.

There was no clear trend in the global CRF over the entire period, and it remained at approximately 45% (figure 1). However, the spatial variability of CRF itself is very large, reaching nearly 80% in tropical regions with high vegetation biomass, and below 10% in arid regions with low biomass (figure 2). There are significant differences depending on land-use types (figure 1). As shown in previous studies (e.g. Yan *et al* 2005), CRF was more pronounced in natural ecosystems than in agricultural ecosystems, with the CRF for soil NO*x* in natural ecosystems accounting for 47.3% of the global annual average, compared with 34.7% in agricultural ecosystems during the simulated period (figure 1). Therefore, land-use conversion to agricultural land is likely to influence global CRF; however, CRF in both natural and agricultural ecosystems showed increasing trends, counteracting the potential reduction associated with land-use conversion. This increase in CRF is attributed to factors such as the accumulation of forest biomass and the resulting increase in LAI, with CRF in natural ecosystems rising from 46.4% before 1900 to 48.8% in the 2010s. In agricultural ecosystems, global CRF has increased significantly since 1950 (from 32.9% to 40.0% in the same period), mainly as a result of the expansion of improved agricultural management practices such as irrigation and fertilization managements (Hurtt *et al* 2020).

3.2. Regional historical trends and the contribution of soil to anthropogenic NO*x* emissions

Regional differences are similar to global trends over the calculation period; however, the trend in soil NO*x* emissions has become more pronounced in some regions since 1950. In particular, significant increases in total soil NO*x* emissions were observed in Europe, E. Asia, S. Asia, S.E. Asia, and temperate N. America (figure 3). In contrast, increases were not obvious in other regions. In regions where increases were observed, the increase in NO*x* emissions from the agricultural ecosystem (figure S3) resulting from the cropland expansion and increased use of chemical N fertilizers considerably contributed to this increase. Notably, in Europe and S. Asia, over half of soil NO*x* emissions originated from agricultural land. Following these regions, the proportion of agricultural land-derived NO*x* was high in Temperate N. America and E Asia in the 21st century. Notably, soil NO*x* emissions from agricultural land in Europe and B. Asia have been peaked out since 1990, accompanied by changes in chemical N fertilizer use (Tian *et al* 2022).

In tropical rainforests such as those in C. America, Tropical S. America, C. Africa and S.E. Asia, high CRFs (figure 3) were observed, with more than 70% of soil NO*x* emissions attenuated by the canopy (figure 2). This substantial attenuation is attributable to the high LAI of vegetation canopies in these regions. Although soil NO_x emissions in tropical rainforests were significantly higher than in other regions—often exceeding 20 Gg N per grid cell due to high temperatures—ecosystem-level NO_x emissions remain relatively low because of strong canopy uptake, with only a few grids surpassing this value (figure 2). In contrast, ecosystems classified as steppe or shrubland, located in temperate or arid zones, have low LAI and thus a lower CRF. Therefore, regions such as Temperate North America (period average 28.1%) and Western Asia (period average 21.1%), where these ecosystems are distributed, have low CRF as a result. Additionally, in W. Asia, agricultural ecosystems have higher CRF values than natural ecosystems (25.4% and 19.3%, respectively) in our simulation because the LAI is higher in agricultural land. However, previous studies using MODIS LAI have also pointed out that irrigated agricultural land has a higher LAI than natural ecosystems (Singh *et al* 2018); therefore, the conversion of land-use to agricultural ecosystems has contributed to an increase in CRF. As such, the effects of land-use change vary depending on the original ecosystem type, so it is important to consider

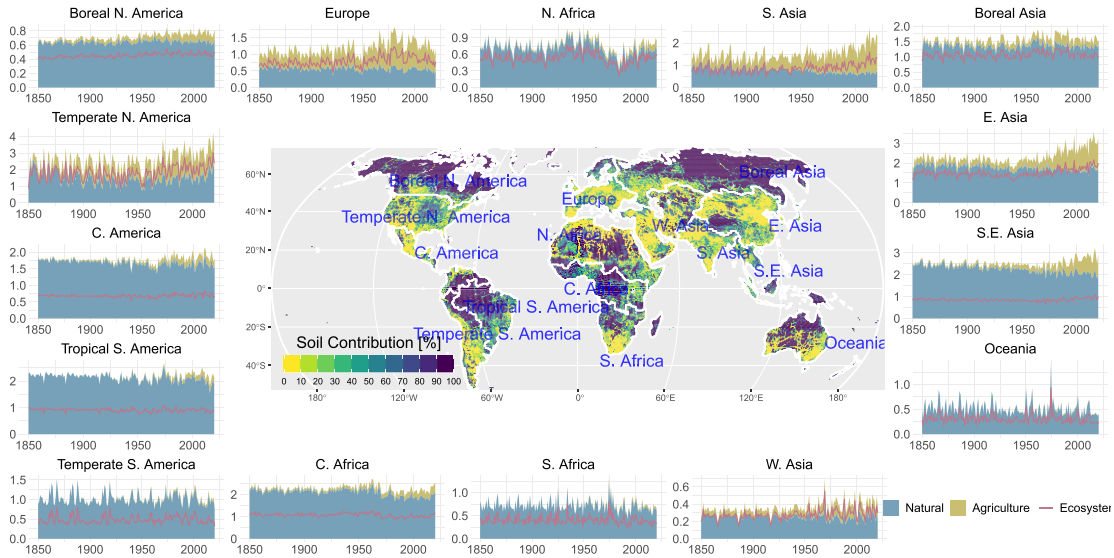


Figure 3. Historical trends in regional soil NO*x* emissions (Tg N) and the map of soil NO*x* contribution to total NO*x* emissions (percentage) in land. The white lines indicate the border for 15 regions, which is defined in the RECCAPP2 study. For NO*x* emissions in other sectors, we used EDGAR HTAPv3 (Crippa *et al* 2023).

regional characteristics when evaluating the impacts of land-use change.

Finally, we compared simulated soil NO*x* emissions (above canopy) with anthropogenic NO*x* emissions from land sources other than soil in EDGAR HTAP3 (i.e. excluding emissions from shipping, aviation, and agriculture) (Crippa *et al* 2018). The annual emissions from sources other than soil in EDGAR HTAP3 averaged 30.8 Tg N yr^{-1} from 2010 to 2015 (converted to N weight as NO_2 in this case). The map in figure 3 shows the fraction of soil NO*x* (above canopy) to the total NO*x* emissions in each grid cell. In the areas of boreal N. America and boreal Asia, which has a low human populations, soil NO*x* emissions are predominant, with values approaching nearly 100% in some areas. Also, in regions such as the Sahara Desert, Central Asia, and the Australian interior, anthropogenic NO*x* emissions from fossil fuel combustion are limited, resulting in a relatively high share of naturally occurring NO emissions from dry soils. Furthermore, sparse vegetation means that there is less canopy NO*x* attenuation (figure 1), which further enhances the relative contribution of soil-derived NO*x* in these arid areas. Mountainous areas have also been identified as regions where nearly 100% of NO*x* originates from the soil (Molina-Herrera *et al* 2017). This cannot be highlighted in our simulation because we used a coarse spatial resolution of the 0.5 grid.

In regions with moderate to high population densities, such as temperate N. America, Europe, S. Asia, and E. Asia, anthropogenic sources other than soil play an important role, but a certain contribution has been observed. Regions where the contribution exceeds 30% in the moderately to highly populated areas include, for example, the Corn Belt in the United States and grain-producing regions in Europe. In these regions, soil NO*x* derived from agricultural land dominates over that of natural ecosystems, suggesting that agricultural activities significantly influence air quality as show in previous regional studies Almaraz *et al* (2018), Skiba *et al* (2021), e.g. Note that the average soil NO*x* emissions for the comparison period in the original EDGAR data were 1.4 Tg N (converted to N weight as NO in this case) (Crippa *et al* 2018), while the results from VISIT were 4.6 Tg N, indicating a notably higher value. Our results underscores the role of agricultural NO emissions enhanced by fertilizer application and land management practices in cultivated systems. Together, these findings stress the need for region-specific mitigation strategies. While fossil fuel reduction remains key in urban areas, targeted agricultural nitrogen management is equally crucial for lowering soil NO*x* emissions in intensively farmed regions.

3.3. Benchmarking using model inter-comparison study for global soil NO*x* emissions

In the terrestrial biogeochemical models in the NMIP2 study (Tian *et al* 2024), global soil surface NO*x* emissions showed a large divergence over the entire simulation period (figure 4). However, with the exception of the ISAM model, the amount of soil NO*x* emissions were generally comparable to those reported in previous studies during the 1990s and 2000s (table 1). The time-series of global soil NO*x* emission based on the ensemble average of all models (geometric mean) was 9.99 Tg N yr^{-1} before 1900 and 16.1 Tg N yr^{-1} in the 2010s. Although VISIT is within the 95% interval, soil NO*x* emissions in VISIT are the second largest among NMIP2 models. Regarding global N_2O emissions, the NMIP2 model

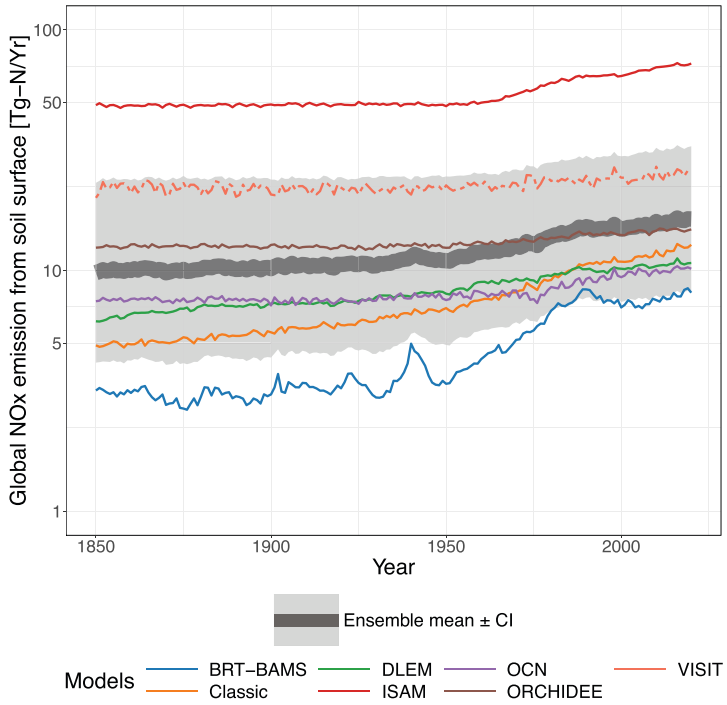


Figure 4. Global soil NO*x* emissions (from soil surface) in NMIP2 models. Colors (except red) in the lines indicate the model. The black line and gray envelope indicate the mean and 95% confidence interval among the models.

results converged well, with all models falling within the range of 10–14 Tg N yr^{-1} by the 2010s (Tian *et al* 2024). However , soil NO*x* emissions in the 2010s showed a considerable variation among the models, ranging from 7.8 Tg N yr^{-1} to 71.0 Tg N yr^{-1}. When examining the increments from the 1850s to the 2010s, there was a large variation, ranging from 2.2 to 22.6 Gg N yr^{-1} (6.1 Gg N yr^{-1} in ensemble average). The percentage increase ranged from 14.2% to 150.6% (ensemble average of 60.6%), which clearly indicates the significant differences in sensitivity to land-use changes and chemical fertilizer inputs. The increment in VISIT during the same period was 3.1 Tg N, the third smallest value of the NMIP2 models. Key parameters influencing NO emissions include soil N availability, temperature dependence, moisture dependence, and pH sensitivity (e.g. Pilegaard 2013). However, to enhance the reliability of future projections, improving the comprehensive nitrogen budget within biogeochemical models—considering both nitrogen inputs and outputs in natural ecosystems and agricultural ecosystems—is a crucial first step. From this perspective, the model with high emissions requires significant improvements in its estimation of soil NO*x* emissions.

Future improvements should focus on expanding atmospheric inversion studies and satellite-based constraints to refine soil NO_x estimates in biogeochemical models, especially in under-sampled regions. NO*x* observation satellites (Miyazaki and Bowman 2023), such as OMI-2 (Levelt *et al* 2006), GOME (Callies *et al* 2000), and more recently GOSAT-GW (Tanimoto *et al* 2025), are important for inverse analysis methods and the separation of emission sources. However, inverse analysis can only determine the net flux attenuated by the forest canopy, so soil flux observations using such chamber methods are important. Global databases similar to those established for GHG fluxes (e.g. SRDB (Jian *et al* 2021)) may also be necessary. The biome-scale emission intensities simulated by VISIT generally fall within the range reported by field observations summarized in Stehfest and Bouwman (2006) (figure S1 and table S1). However, one-to-one verification at individual observation sites has not been performed. Therefore, reconstructing spatial grid estimates using machine learning with monitoring network data is likely to be useful for validating surface soil NO*x* fluxes in biogeochemical models, also significant for bridging these gaps.

It will also be important to set parameters and develop models based on observations for the CRF scheme (Delaria *et al* 2018). Supplementary sensitivity experiments indicate that uncertainties in the CRF parameters translate into moderate but systematic uncertainty in global soil NO_x emissions. A ±20% perturbation of k_s resulted in a −3.96% to +4.40% change in the global CRF, corresponding to −0.51 to +0.57 Tg N yr^{-1} in NO_x emissions, while k_c produced a similar range (−4.26% to +5.51%; −0.55 to +0.71 Tg N yr^{-1}). Although these sensitivities remain moderate, they highlight a structural limitation of current large-scale models. Most global biogeochemical models adopt simplified 'big-leaf'

canopy representations with empirically derived coefficients that were originally constrained by limited observations. Yet canopy-atmosphere exchange depends on turbulence, chemistry, and vegetation structure, which remain poorly constrained in both models and measurements (Ganzeveld *et al* 2002, Visser *et al* 2022). Improving CRF parameterizations therefore requires coordinated advances in process-based modeling and expanded canopy-scale observations of NO_x exchange. Future work should also consider the role of seasonal vegetation dynamics and phenology, as temporal variations in canopy structure and leaf development may modulate the effective attenuation of soil NO_x emissions and introduce additional variability in CRF.

Uncertainties in anthropogenic nitrogen input datasets could also be an uncertainty source of soil NO*x* emissions. However, long-term, spatially explicit datasets covering the historical simulation period for global fertilizer and livestock manure inputs remain limited. The HaNi dataset (Tian *et al* 2022) is one of the few harmonized reconstructions suitable for long-term global simulations. Nevertheless, significant uncertainties persist in current nitrogen input datasets, both in the global agricultural nitrogen input data itself and in the nitrogen budget within agricultural ecosystems (Zhang *et al* 2021), potentially introducing uncertainty into global soil NO*x* emissions. Reducing the uncertainty in nitrogen input data and improving the nitrogen budget in agricultural ecosystems are essential for enhancing the accuracy of global Soil NO*x* emissions.

Despite these limitations, our century-scale simulation fills a critical knowledge gap by providing a continuous historical perspective that is not achievable through observations alone. The use of the harmonized HaNi nitrogen input dataset and the integration of canopy attenuation processes further enhance the robustness of our long-term estimates. This contributes essential boundary conditions for atmospheric chemistry modeling and supports the development of region-specific nitrogen management strategies. Furthermore, to improve model accuracy in arid and semi-arid regions such as sub-Saharan Africa, reproducing spike NO*x* emissions—which were omitted in this study—remains a future challenge. Globally, such pulse events are estimated to account for about 4% of the annual soil NO*x* budget (Yan *et al* 2005), which is not so large from the view to the assessment for land-use change at global scale in this study. However, in seasonally arid ecosystems, capturing these sudden emission events at finer resolution is necessary (Zörner *et al* 2016, Hickman *et al* 2021). Recent high-frequency observations indicate that rainfall-induced NO*x* surges are extremely short-lived. Initial peaks occur within 30 min, and the main emission phase often concludes within a day to several days (Hickman *et al* 2021, Slessarev *et al* 2021). Improving VISIT model's predictive performance will require the implementation of higher temporal resolution and improved representation of arid soil moisture dynamics, which are currently constrained by the coarse spatial resolution inherent in global biogeochemical models (Yan *et al* 2005).

3.4. Conclusions

This study demonstrated that global NO*x* emissions have increased as a result of the conversion of natural ecosystems into agricultural land. The conversion of natural ecosystems into agricultural land led to a shift in dominant soil NO*x* emission sources, resulting in an increase of approximately 3.1 Tg N at the global soil surface.

Our global assessment highlights the spatial heterogeneity of soil NO*x* emission dynamics accompanied by land-use change over long-term periods. In areas with low population density, NO*x* emissions from soil are dominant in each region. However, even in densely populated areas, NO*x* emissions from natural ecosystems and agricultural soils are quantitatively important. Furthermore, as revealed by regional analysis, it has become clear that the land-use changes accompanied with the chemical N fertilizer and manure uses has been the dominant factor driving the increasing trend of soil NO*x* in North America, Europe, and Asian regions during the period from 1850 to 2020. This study also quantitatively demonstrated that the attenuation of soil NO*x* by the vegetation canopy is a dominant factor influencing regional Soil NO*x* emission levels. This is also important for understanding the impacts of land-use changes, an aspect that has not been extensively addressed in previous studies.

As future emissions of fossil fuel-derived NO*x* are reduced, the importance of soil NO*x* emissions associated with land-use and agricultural management will grow increasingly significant. Various future scenarios have been proposed regarding the expansion of cropland to produce food and bioenergy crops to meet the increased demand by population growth (Kanter *et al* 2020, Chang *et al* 2021), which will increase chemical N fertilizer and manure applications and promote soil NO*x* emissions. To improve the predictions for NO*x* to inform atmospheric chemistry and climate change, it is more necessary to improve the prediction performance of biogeochemical models for future projections.

Acknowledgments

This study was conducted based on NMIP2 protocol, and we would like to express our sincere gratitude to the contributors to NMIP2 activities. This study conducted as part of the JpNwst project, which was

funded by the Environment Research and Technology Development Fund (JPMEERF20235001) of the Environmental Restoration and Conservation Agency (ERCA) provided by Ministry of the Environment of Japan. K N were also partially supported by JPMEERF21S12000 of ERCA. The authors used ChatGPT (OpenAI) for English language editing and readability improvement during manuscript preparation.

Data availability statement

The data that support the findings of this study are openly available at the following URL/DOI: https://doi.org/10.17595/20260428.001 (Nishina 2026).

Supplementary material available at: https://doi.org/10.1088/1748-9326/ae6c3a/data1.

Author contributions

Kazuya Nishina 0000-0002-8820-1282
Conceptualization (lead), Formal analysis (lead), Funding acquisition (equal), Investigation (lead), Methodology (lead), Project administration (equal), Software (lead), Visualization (lead), Writing – original draft (lead)

Akihiko Ito 0000-0001-5265-0791
Methodology (equal), Software (equal), Writing – review & editing (equal)

Hanqin Tian 0000-0002-1806-4091
Conceptualization (lead), Data curation (lead), Methodology (lead), Writing – review & editing (equal)

Tatsuya Nagashima
Writing – review & editing (equal)

Yuto Osugi
Software (equal), Writing – review & editing (equal)

Naiqing Pan 0000-0002-1465-7738
Data curation (equal), Methodology (equal), Writing – review & editing (equal)

Shufen Pan 0000-0001-7920-1427
Data curation (equal), Methodology (equal), Writing – review & editing (equal)

Sian Kou-Giesbrecht 0000-0002-4086-0561
Formal analysis (equal), Writing – review & editing (equal)

Federico Maggi 0000-0002-7878-8112
Formal analysis (equal), Writing – review & editing (equal)

Atul K Jain 0000-0002-4051-3228
Formal analysis (equal), Writing – review & editing (equal)

Nicolas Vuichard
Formal analysis (equal), Writing – review & editing (equal)

Sönke Zaehle 0000-0001-5602-7956
Formal analysis (equal), Writing – review & editing (equal)

References

Ainsworth E A and Long S P 2005 What have we learned from 15 years of free-air CO_2 enrichment (FACE)? A meta-analytic review of the responses of photosynthesis, canopy properties and plant production to rising CO_2 *New Phytol.* **165** 351–72

Almaraz M, Bai E, Wang C, Trousdell J, Conley S, Faloona I and Houlton B Z 2018 Agriculture is a major source of NOx pollution in California *Sci. Adv.* **4** eaao3477

Atkinson R 2000 Atmospheric chemistry of VOCs and NOx *Atmos. Environ.* **34** 2063–101

Atkinson R, Baulch D L, Cox R A, Crowley J N, Hampson R F, Hynes R G, Jenkin M E, Rossi M J and Troe J 2004 Evaluated kinetic and photochemical data for atmospheric chemistry: volume I—gas phase reactions of O_x, HO_x, NO_x and SO_x species *Atmos. Chem. Phys.* **4** 1461–738

Bouwman A F, Boumans L J M and Batjes N H 2002 Modeling global annual N_2O and NO emissions from fertilized fields *Glob. Biogeochem. Cycles* **16** 1080

Callies J, Corpaccioli E, Eisinger M, Hahne A and Lefebvre A 2000 GOME-2-Metop's second-generation sensor for operational ozone monitoring *ESA Bull.* **102** 28–36 (available at: www.esa.int/esapub/bulletin/bullet102/Callies102.pdf)

Chang J, Havlík P, Leclère D, de Vries W, Valin H, Deppermann A, Hasegawa T and Obersteiner M 2021 Reconciling regional nitrogen boundaries with global food security *Nat. Food* **2** 700–11

Chatani S, Shimadera H, Kitayama K and Nishina K 2025 Numerical analysis of factors causing long-term trends and annual variations of sulfur and nitrogen deposition amount in Japan from 2000 to 2020 *Asian J. Atmos. Environ.* **19** 2

Christiansen A, Mickley L J and Hu L 2024 Constraining long-term NOx emissions over the United States and Europe using nitrate wet deposition monitoring networks *Atmos. Chem. Phys.* **24** 4569–89

Crippa M *et al* 2018 Gridded emissions of air pollutants for the period 1970–2012 within EDGAR v4.3.2 *Earth Syst. Sci. Data* **10** 1987–2013

Crippa M *et al* 2023 The HTAP_v3 emission mosaic: merging regional and global monthly emissions (2000–2018) to support air quality modelling and policies *Earth Syst. Sci. Data* **15** 2667–94

Davidson E A and Kingerlee W 1997 A global inventory of nitric oxide emissions from soils *Nutr. Cycl. Agroecosyst.* **48** 37–50

Delaria E R, Vieira M, Cremieux J and Cohen R C 2018 Measurements of NO and NO_2 exchange between the atmosphere and *Quercus agrifolia Atmos. Chem. Phys.* **18** 14161–73

Derwent R, Stevenson D, Doherty R, Collins W, Sanderson M and Johnson C 2008 Radiative forcing from surface NOx emissions: spatial and seasonal variations *Clim. Change* **88** 385–401

Feng Z, Kobayashi K and Ainsworth E A 2008 Impact of elevated ozone concentration on growth, physiology and yield of wheat (*Triticum aestivum* L.): a meta-analysis *Glob. Change Biol.* **14** 2696–708

Ganzeveld L N, Lelieveld J, Dentener F J, Krol M C, Bouwman A J and Roelofs G-J 2002 Global soil-biogenic NOx emissions and the role of canopy processes *J. Geophys. Res. Atmos.* **107** ACH 9–1–17

Gong C, Tian H, Liao H, Pan N, Pan S, Ito A, Jain A K, Kou-Giesbrecht S, Joos F and Sun Q *et al* 2024 Global net

climate effects of anthropogenic reactive nitrogen *Nature* **632** 557–63
Gregg J W, Jones C G and Dawson T E 2003 Urbanization effects on tree growth in the vicinity of New York city *Nature* **424** 183–7
Harris I C 2021 CRU JRA v2.2: a forcings dataset of gridded land surface blend of Climatic Research Unit (CRU) and Japanese reanalysis (JRA) data *NERC EDS Centre for Environmental Data Analysis* (available at: https://catalogue.ceda.ac.uk/uuid/4bdf41fc10af4caaa489b14745c665a6)
Hegglin M, Kinnison D and Lamarque J F 2016 CCMI nitrogen surface fluxes in support of CMIP6 - version 2.0. Version *Earth System Grid Federation* (https://doi.org/10.22033/ESGF/input4MIPs.1125)
Hickman J E, Kaya B, Kebede A, Kandji S, Fitch L, Neill C, Nyadzi G, Diru W and Palm C A 2021 Little effect of land use on N_2O and NO emission pulses following rewetting of dry soils across seasonally dry sub-Saharan Africa *J. Geophys. Res. Biogeosci.* **126** e2020JG005742
Hudman R, Moore N, Mebust A, Martin R, Russell A, Valin L and Cohen R 2012 Steps towards a mechanistic model of global soil nitric oxide emissions: implementation and space based-constraints *Atmos. Chem. Phys.* **12** 7779–95
Hurtt G C *et al* 2020 Harmonization of global land use change and management for the period 850–2100 (LUH2) for CMIP6 *Geosci. Model Dev.* **13** 5425–64
Ito A 2018 Disequilibrium of terrestrial ecosystem CO_2 budget caused by disturbance-induced emissions and non-CO_2 carbon export flows: a global model assessment *Earth Syst. Dyn.* **10** 685–709
Ito A 2019 Methane emission from pan-Arctic natural wetlands estimated using a process-based model, 1901–2016 *Polar Sci.* **20** 105–15
Ito A and Inatomi M 2011 Water-use efficiency of the terrestrial biosphere: a model analysis focusing on interactions between the global carbon and water cycles *J. Hydrometeorol.* **13** 681–94
Jacob D J, Wofsy S C, Bakwin P S, Fan S-M, Harriss R C and Talbot R W 1995 Deposition of ozone to vegetation: an overview *J. Geophys. Res. Atmos.* **100** 21163–78
Jian J *et al* 2021 A restructured and updated global soil respiration database (SRDB-V5) *Earth Syst. Sci. Data* **13** 255–67
Joos F and Spahni R 2008 Rates of change in natural and anthropogenic radiative forcing over the past 20,000 years *Proc. Natl Acad. Sci. USA* **105** 1425–30
Kanter D R *et al* 2020 A framework for nitrogen futures in the shared socioeconomic pathways *Glob. Environ. Change* **61** 102029
Kou-Giesbrecht S and Arora V K 2023 Compensatory effects between CO_2, nitrogen deposition and nitrogen fertilization in terrestrial biosphere models without nitrogen compromise projections of the future terrestrial carbon sink *Geophys. Res. Lett.* **50** e2022GL102618
Lan X, Tans P and Thoning K 2023 Trends in globally-averaged CH_4, N_2O, and SF_6 determined from NOAA global monitoring laboratory measurements Version 2023-03 (https://doi.org/10.15138/P8XG-AA10)
Levelt P, Hilsenrath E, Leppelmeier G, van den Oord G, Bhartia P, Tamminen J, de Haan J and Veefkind J 2006 Science objectives of the ozone monitoring instrument *IEEE Trans. Geosci. Remote Sens.* **44** 1199–208
Lin X *et al* 2024 European soil NOx emissions derived from satellite NO_2 observations *J. Geophys. Res. Atmos.* **129** e2024JD041492
Liu S, Lin F, Wu S, Ji C, Sun Y, Jin Y, Li S, Li Z and Zou J 2017 A meta-analysis of fertilizer-induced soil NO and combined NO+N_2O emissions *Glob. Change Biol.* **23** 2520–32
Melton J R, Arora V K, Wisernig-Cojoc E, Seiler C, Fortier M, Chan E and Teckentrup L 2020 CLASSIC v1.0: the open-source community successor to the Canadian Land Surface Scheme (CLASS) and the Canadian Terrestrial Ecosystem Model (CTEM)—part 1: model framework and site-level performance *Geosci. Model Dev.* **13** 2825–50
Miyazaki K and Bowman K 2023 Predictability of fossil fuel CO_2 from air quality emissions *Nat. Commun.* **14** 1604
Miyazaki K, Eskes H, Sudo K, Boersma K F, Bowman K and Kanaya Y 2017 Decadal changes in global surface NOx emissions from multi-constituent satellite data assimilation *Atmos. Chem. Phys.* **17** 807–37
Molina-Herrera S *et al* 2017 Importance of soil NO emissions for the total atmospheric NOx budget of saxony, germany *Atmos. Environ.* **152** 61–76
Nishina K 2026 Simulated Global Soil NOx emissions using VISIT model *Global Environmental Database (GED)* (https://doi.org/10.17595/20260428.001)
Nishina K, Akiyama H, Nishimura S, Sudo S and Yagi K 2012 Evaluation of uncertainties in N_2O and NO fluxes from agricultural soil using a hierarchical Bayesian model *J. Geophys. Res. Biogeosci.* **117** G04008
Nishina K, Takenaka C and Ishizuka S 2009 Relationship between N_2O and NO emission potentials and soil properties in Japanese forest soils *Soil Sci. Plant Nutr.* **55** 203–14
Oikawa P, Ge C, Wang J, Eberwein J, Liang L, Allsman L, Grantz D and Jenerette G 2015 Unusually high soil nitrogen oxide emissions influence air quality in a high-temperature agricultural region *Nat. Commun.* **6** 8753
Parton W, Holland E, Del Grosso S, Hartman M, Martin R, Mosier A, Ojima D and Schimel D 2001 Generalized model for NOx and N_2O emissions from soils *J. Geophys. Res. Atmos.* **106** 17403–19
Parton W, Mosier A, Ojima D, Valentine D, Schimel D, Weier K and Kulmala A E 1996 Generalized model for N_2 and N_2O production from nitrification and denitrification *Glob. Biogeochem. Cycles* **10** 401–12
Pasut C, Tang F H M, Hamilton D, Riley W J and Maggi F 2021 Spatiotemporal assessment of GHG emissions and nutrient sequestration linked to agronutrient runoff in global wetlands *Glob. Biogeochem. Cycles* **35** e2020GB006816
Pilegaard K 2013 Processes regulating nitric oxide emissions from soils *Soil Emissions of Nitrous Oxide and Nitric Oxide* (Springer) pp 59–82
Potter C S, Matson P A, Vitousek P M and Davidson E A 1996 Process modeling of controls on nitrogen trace gas emissions from soils worldwide *J. Geophys. Res. Atmos.* **101** 1361–77
Sha T, Ma X, Zhang H, Janechek N, Wang Y, Wang Y, Castro García L, Jenerette G D and Wang J 2021 Impacts of soil NOx emission on O_3 air quality in rural California *Environ. Sci. Technol.* **55** 7113–22
Shu S, Jain A K, Koven C D and Mishra U 2020 Estimation of permafrost SOC stock and turnover time using a land surface model with vertical heterogeneity of permafrost soils *Glob. Biogeochem. Cycles* **34** e2020GB006585
Simpson D and Darras S 2021 Global soil NO emissions for atmospheric chemical transport modelling: CAMS-GLOB-SOIL v2.2 *Earth Syst. Sci. Data Discuss.* **2021** 1–35
Singh D, McDermid S P, Cook B I, Puma M J, Nazarenko L and Kelley M 2018 Distinct influences of land cover and land management on seasonal climate *J. Geophys. Res. Atmos.* **123** 12–017
Skiba U, Medinets S, Cardenas L M, Carnell E J, Hutchings N and Amon B 2021 Assessing the contribution of soil NOx emissions to European atmospheric pollution *Environ. Res. Lett.* **16** 025009
Slessarev E W, Greene A C, Homyak P M, Ying S C and Schimel J P 2021 High resolution measurements reveal abiotic and biotic mechanisms of elevated nitric oxide emission after wetting dry soil *Soil Biol. Biochem.* **160** 108316
Stehfest E and Bouwman L 2006 N_2O and NO emission from agricultural fields and soils under natural vegetation: summarizing available measurement data and modeling of global annual emissions *Nutr. Cycl. Agroecosyst.* **74** 207–28
Steinkamp J and Lawrence M G 2011 Improvement and evaluation of simulated global biogenic soil NO emissions in an AC-GCM *Atmos. Chem. Phys.* **11** 6063–82

Sun Q, Joos F, Lienert S, Berthet S, Carroll D, Gong C, Ito A, Jain A K, Kou-Giesbrecht S and Landolfi A *et al* 2024 The modeled seasonal cycles of surface N_2O fluxes and atmospheric N_2O *Glob. Biogeochem. Cycles* **38** e2023GB008010

Szopa S *et al* 2021 Short-lived climate forcers *IPCC 2021: Climate Change 2021: The Physical Science Basis. Contribution of Working Group I to the Sixth Assessment Report of the Intergovernmental Panel on Climate Change* ed V Masson-Delmotte *et al* (Cambridge University Press) ch 6, pp 817–922

Tanimoto H *et al* 2025 The greenhouse gas observation mission with global observing satellite for greenhouse gases and water cycle (GOSAT-GW): objectives, conceptual framework and scientific contributions *Prog. Earth Planet. Sci.* **12** 8

Tao Z and Jain A K 2005 Modeling of global biogenic emissions for key indirect greenhouse gases and their response to atmospheric CO_2 increases and changes in land cover and climate *J. Geophys. Res. Atmos.* **110** D21309

Tian H *et al* 2015 Global methane and nitrous oxide emissions from terrestrial ecosystems due to multiple environmental changes *Ecosyst. Health Sustain.* **1** 1–20

Tian H *et al* 2020 A comprehensive quantification of global nitrous oxide sources and sinks *Nature* **586** 248–56

Tian H *et al* 2022 History of anthropogenic nitrogen inputs (HaNi) to the terrestrial biosphere: a 5 arcmin resolution annual dataset from 1860 to 2019 *Earth Syst. Sci. Data* **14** 4551–68

Tian H *et al* 2024 Global nitrous oxide budget (1980–2020) *Earth Syst. Sci. Data* **16** 2543–604

Vinken G C, Boersma K F, Maasakkers J D, Adon M and Martin R V 2014 Worldwide biogenic soil NOx emissions inferred from OMI NO2 observations *Atmos. Chem. Phys.* **14** 10363–81

Song W, Liu X Y, Hu C C, Chen G Y, Liu X J, Walters W W, Michalski G and Liu C Q 2021 Important contributions of non-fossil fuel nitrogen oxides emissions *Nat. Commun.* **12** 243

Visser A J, Ganzeveld L N, Finco A, Krol M C, Marzuoli R and Boersma K F 2022 The combined impact of canopy stability and soil NOx exchange on ozone removal in a temperate deciduous forest *J. Geophys. Res. Biogeosci.* **127** e2022JG006997

Vuichard N, Messina P, Luyssaert S, Guenet B, Zaehle S, Ghattas J, Bastrikov V and Peylin P 2019 Accounting for carbon and nitrogen interactions in the global terrestrial ecosystem model orchidee (trunk version, rev 4999): multi-scale evaluation of gross primary production *Geosci. Model Dev.* **12** 4751–79

Weng H *et al* 2020 Global high-resolution emissions of soil NOx, constrained by OMI satellite observations *Sci. Data* **7** 148

Xu R, Tian H, Lu C, Pan S, Chen J, Yang J and Zhang B 2017 Preindustrial nitrous oxide emissions from the land biosphere estimated by using a global biogeochemistry model *Clim. Past* **13** 977–90

Yan X, Ohara T and Akimoto H 2005 Statistical modeling of global soil NOx emissions *Glob. Biogeochem. Cycles* **19** GB3019

Yienger J J and Levy H 1995 Empirical model of global soil-biogenic NOx emissions *J. Geophys. Res. Atmos.* **100** 11447–64

Zaehle S and Friend A D 2010 Carbon and nitrogen cycle dynamics in the O-CN land surface model: 1. Model description, site-scale evaluation and sensitivity to parameter estimates *Glob. Biogeochem. Cycles* **24** GB1005

Zhang X, Zou T, Lassaletta L, Mueller N D, Tubiello F N, Lisk M D, Lu C, Conant R T, Dorich C D and Gerber J *et al* 2021 Quantification of global and national nitrogen budgets for crop production *Nat. Food* **2** 529–40

Zörner J, Penning de Vries M, Beirle S, Sihler H, Veres P R, Williams J and Wagner T 2016 Multi-satellite sensor study on precipitation-induced emission pulses of NOx from soils in semi-arid ecosystems *Atmos. Chem. Phys.* **16** 9457–87